

On Prediction of Record-Breaking Daily Temperature Events*

FENG Guolin^{1,2,3†}(封国林), YANG Jie^{1,2}(杨杰), WAN Shiquan⁴(万仕全), HOU Wei^{1,3}(侯威),
and ZHI Rong^{1,2}(支蓉)

¹ College of Physical Science and Technology, Yangzhou University, Yangzhou 225002

² State Key Laboratory of Earth Surface Processes and Resource Ecology, College of Global Change and Earth System Science, Beijing Normal University, Beijing 100875

³ Key Laboratory of Regional Climate-Environment for Temperate East Asia, Institute of Atmospheric Physics, Chinese Academy of Sciences, Beijing 100029

⁴ Yangzhou Meteorological Bureau, Yangzhou 225009

(Received April 22, 2009)

ABSTRACT

The daily maximum/minimum temperature data at 740 stations in China from 1960 to 2005 were analyzed to reveal the statistical characteristics of record-breaking (RB) daily extreme temperature events in the past 46 yr. It is verified that the observational daily extreme temperatures obey the Gaussian distribution. The expected values of RB extreme temperatures were obtained based on both the Gaussian distribution model and the initial condition of observed historical RB high/low temperature events after tedious theoretical derivation. The results were then compared with those obtained by the iteration computation of the pure theoretical model. The comparison suggests that the results from the former are more consistent with the observations than those from the latter. Based on the above analyses, prediction of future possible RB high/low temperature events is made, and the spatial distributions of maximum/minimum theoretical values of their intensities are also given. It is indicated that the change amplitudes of future extreme temperatures differ evidently from place to place, showing a remarkable regional feature: the future extremely high temperature events will have a strong rising intensity in Southwest China, and a relatively weak rising intensity in western China; while the largest decrease of the future extremely low temperature events will appear in Northeast China and the north of Northwest China, and the decrease will be maintained relatively stable in space in Central China and Southwest China, in comparison with the historical low temperature pattern. Features in the occurrence time of the future RB temperature events are also illustrated.

Key words: record-breaking, extreme temperature, prediction of extreme event

Citation: Feng Guolin, Yang Jie, Wan Shiquan, et al., 2009: On prediction of record-breaking daily temperature events. *Acta Meteor. Sinica*, **23**(6), 666–680.

1. Introduction

Temperature is one of the important indices in climate change research, and its change impacts greatly the human production activities and the natural environment (Render and Petersen, 2006; Qin et al., 2007). In the recent 100 yr, global climate is undergoing a distinctive warming. Frequent extreme climate events have changed the global natural ecological systems and the economy and life of human society, thus becoming one of the severe challenges to the sustainable development of human society. These have attracted increasing public attention on extreme temperatures (Liu et

al., 2006; Ye et al., 2006). However, prediction of extreme events is still a scientific crux due to lack of observational data and prediction methods. Our understanding of the change of extreme climate, e.g., how the climate change affects the occurrence and development of extreme temperature events and how the extreme temperatures respond to the climate change, is rather insufficient relative to the mean climate change (Ding et al., 2006). Global warming renders regional extreme climate events more severe and their frequencies and amplitudes more complicated (Feng et al., 2006; Hou et al., 2006). Therefore, study on the evolutionary laws of the intensity and frequency of

*Supported by the National Science and Technology Support Program of China under Grant No. 2007BAC29B01, the National Basic Research Program of China under Grant No. 2006CB400503, the National Natural Science Foundation of China under Grant No. 40875040, and the Special Project for Public Welfare under Grant No. GYHY200806005.

†Corresponding author: fenggl@cma.gov.cn.

record-breaking (RB) temperature events is undoubtedly of applicable value and scientific significance. At present, general circulation models are able to simulate changes in the mean climate on a large scale, but can do little on changes in climatic variables on small- and meso-scale, especially in extreme climate on a regional scale. Thereby, studying the statistical characteristics such as probability of regional extreme climatic events and indirectly predicting their future changes have an important practical meaning. For example, the size of the change amplitude of extreme temperatures can be described using their probability distribution models (Deng et al., 2000; Ding et al., 2004).

RB temperature events are defined as some specific extreme value processes of the temperature distribution. If the statistical objects are extreme temperatures (Sugihara and May, 1990; Fu and Ye, 1995; Liu et al., 2000; Yang and Zhou, 2005), then the defined RB events are one of the extreme events. However, in many cases, RB events are not equal to extreme events. Studies on RB temperature events are of great values. It can reveal the evolutionary laws of extreme temperatures, especially under the background of global warming. RB extreme high temperature events may lead to more severe meteorological disasters, such as megatherm and heat waves (Kiktev et al., 2003; Wan et al., 2005; Beniston et al., 2007). Meanwhile, examinations of RB temperatures may from a new angle of view disclose the evolutionary law of global warming and predict the extreme values of possible high/low temperatures.

2. Data

The daily maximum/minimum temperatures at 583 stations were selected based on the requirement of data continuity from the climate dataset of 740 stations in China from 1960 to 2005, released by China Meteorological Administration. Missing data for a few selected stations were interpolated based on the daily maximum/minimum temperatures of the neighboring stations with consideration of the distance to the station. The selected maximum/minimum temperature data can be written into maximum/minimum temperature time series for each day of the year (365 days;

i.e., a leap year was treated as a normal year), whose sizes are all 46 (1960–2005), and their anomaly time series, denoted respectively as $i = 1, 2, \dots, 365$; $j = 1960, 1961, \dots, 2005$, and X_H/X_L briefly hereafter.

3. Probability theory for RB events

3.1 RB events

RB high temperature events are illustrated by dots on the dashed line in Fig. 1, and the associated probability theory used for RB events was given by Render and Petersen (2006).

Each time a record high for a fixed day of the year t_i is set, we document it as the i th record with the intensity of corresponding record high temperature at T_i . Suppose that the probability density function of series X_H is $p(T)$, and its range is $(+\infty, -\infty)$, then the initial RB high temperature event is defined by the mean value of the series $T_0 \equiv \int_{-\infty}^{\infty} Tp(T)dT$. When the next RB high temperature event $T_1 (> T_0)$ occurs, the probability density function becomes $p_1(T)$, and the variable range becomes $(T_0, +\infty)$. Therefore, to satisfy the normalized condition of probability density function, $p_1(T)$ and $p(T)$ must have the following relation:

$$p_1(T) = \frac{1}{\int_{T_0}^{\infty} p(T)dT} p(T), \quad T \in (T_0, +\infty). \quad (1)$$

Therefore, the expected value of the first RB high

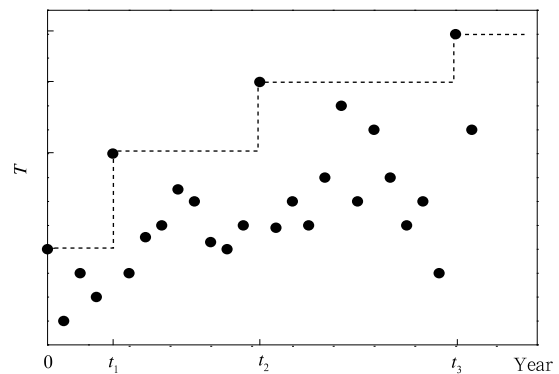


Fig. 1. Schematic evolution of the RB high temperature events (dots on the dashed line) on a specific day. Dots below the dashed line represent the daily high temperature for different years.

temperature event $T_1(> T_0)$ is defined as

$$T_1 \equiv \int_{T_0}^{\infty} T p_1(T) dT = \frac{\int_{T_0}^{\infty} T p(T) dT}{\int_{T_0}^{\infty} p(T) dT}. \quad (2)$$

Its physical meaning is the mean value, or the mathematic expectation of the maximum temperature greater than T_0 . We successively take T_1 as the initial condition for computing the expected value of the second RB high temperature event $T_2(> T_1)$, then T_2 is the mean value of all maximum temperature greater than T_1 . Likewise, the expected value of the $(k + 1)$ th RB high temperature event is defined as

$$T_{k+1} \equiv \frac{\int_{T_k}^{\infty} T p(T) dT}{\int_{T_k}^{\infty} p(T) dT}, \quad (3)$$

where $p(T)$ is the probability density function fitted with the daily high temperature data, rather than one of actual RB high temperature events, because the RB high temperature event defined is a mathematical expectation of the probability distribution of daily high temperature, i.e., a statistical mean, instead of an actual RB high temperature event. For example, we take the average value of all temperatures greater than T_{k-1} in the probability density function of series X_H as T_k , if the size of daily temperature series is determined, then the probability density function in Eqs. (2) and (3) are also correspondingly fixed by fitting. Equations (2) and (3) define the theoretical value of T_k . In fact, Eq. (3) is universal for an arbitrary probability density distribution, thereby, the intensity expectation value series of RB high temperature events can be established, from which we can understand the trend of temperature change from another angle of view.

Two subsidiary distributions needed for record statistics are the probability that a randomly-drawn temperature exceeds T , $p_>(T)$, and the probability that this randomly-selected temperature is less than T , $p_<(T)$. They are defined respectively by

$$p_<(T) \equiv \int_0^T p(T') dT', \quad p_>(T) \equiv \int_T^{\infty} p(T') dT'. \quad (4)$$

In addition to the intensity of record temperatures, we determine the time interval between two

successive records. Suppose that the value of the current (k th) RB high temperature equals T_k , and let $q_n(T_k)$ be the probability that a new record high—the $(k + 1)$ th—is set n -yr later. For this new record, the first $n-1$ highs after the current record must all be less than T_k , while the n th high temperature must exceed T_k . Thus

$$q_n(T_k) = p_<(T_k)^{n-1} p_>(T_k). \quad (5)$$

In the current empirical study, statistics are performed for the same day of each year. Therefore, each series is consisted of temperatures on the same day of different years, the time interval between T_k and T_{k+1} must be the integer times of year. The probability is $p_>$ for the interval of 1 yr, $p_<p_>$ for 2 yr, $p_<^2 p_>$ for 3 yr, and $p_<^{n-1} p_>$ for n yr. Therefore, the expected value of the time interval between the occurrence of the k th and $(k + 1)$ th RB high temperature events is

$$t_{k+1} - t_k = p_> + 2p_<p_> + 3p_<^2 p_> + \dots + np_<^{n-1} p_> = \sum_{n=1}^{\infty} np_<^{n-1} p_>. \quad (6)$$

Obviously, using

$$\int_0^p \sum_{n=1}^{\infty} np^{n-1} dp = \sum_{n=1}^{\infty} \int_0^p np^{n-1} dp = \sum_{n=1}^{\infty} p^n = \frac{p}{1-p}, \quad |p| < 1, \quad (7)$$

the following relation can be derived,

$$\sum_{n=1}^{\infty} np^{n-1} = \left(\frac{p}{1-p}\right)' = \frac{1}{(1-p)^2}, \quad (-1 < p < 1). \quad (8)$$

Therefore, the expected value of the time interval between T_k and T_{k+1} is

$$t_{k+1} - t_k = \sum_{n=1}^{\infty} np_<^{n-1} p_> = \frac{1}{(1-p_<)^2} p_> = \frac{1}{p_>} p_> = \frac{1}{p_>(T_k)}. \quad (9)$$

3.2 Probability distribution models for series X_H/X_L

Many studies suggest that the probability distribution models similar with $p(T)$ in this paper are

generally subject to the unimodal bell-shaped distribution, such as normal distribution, logarithmic normal distribution, Γ distribution, β distribution, Weibull distribution, Gumbel distribution, etc., which are able to fit various biased and unbiased distributions. Among them, the parameter estimation is complicated in fitting the positively biased distribution by the Γ distribution, and in fitting the negatively biased distribution by the β distribution. It is relatively easy in fitting the distributions with a zero or near zero skewness by the normal distribution (Ding et al., 2004; Gong et al., 2006a). We take Nanjing X_H as an example to explore the type of probability density function suitable to our case. Because the size of series X_H is 46, the small sample leads to the larger fluctuations of the fitted distribution curve. To overcome the limitation of insufficient samples and to ensure the accuracy of fitted probability density distribution function, the following data processing was performed. We take 15 January, April, June, and October respectively as rep-

resentative days for winter, spring, summer, and autumn, and the size of series X_H for 15th January as an example is also 46. Based on the fact that temperature series have better persistency and continuity, an assumption was made that the daily high temperatures of the 15 days before and after 15 January for each year are viewed as the temperature on that day to mitigate the insufficiency of samples, and then a simple smoothing was performed on the series. This processing method is relatively rough, but without losing a general reasonability. The size of expanded high temperature series for 15 January is 1426 (46×31), and likewise the similar processing was also performed on series X_H for other seasons.

Figure 2 shows the probability density distributions and corresponding Gaussian fittings of daily high temperature for 15 January, April, June, and October. It is seen from the figure that the range of X_H is larger for 15 January and April, next larger for October, and the smallest for June. The probability density

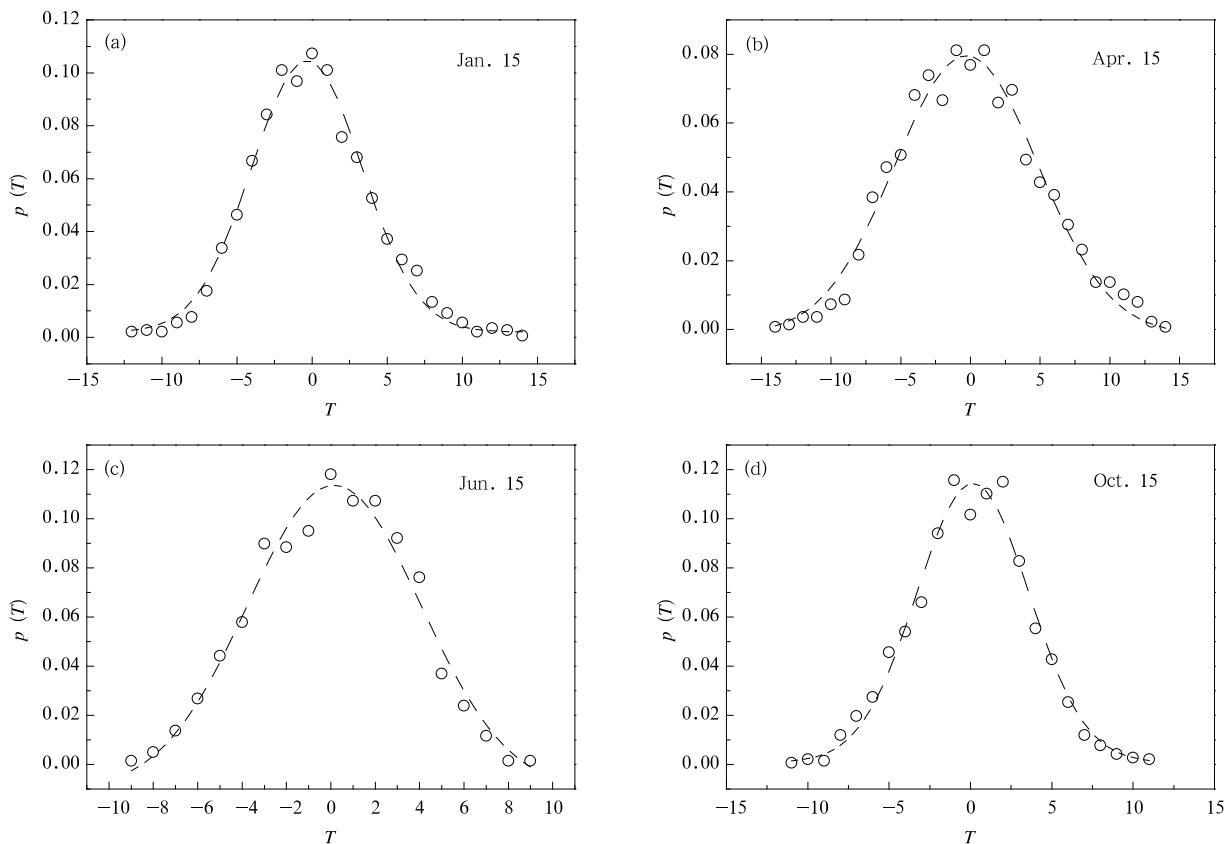


Fig. 2. Probability density distributions (dots) and Gaussian fittings (dashed line) of daily maximum temperature at Nanjing station on 15 (a) January, (b) April, (c) June, and (d) October.

distributions of the four dates are all well consistent with a Gaussian distribution with its maximum value being about 0.1. Likewise, similar fittings of series X_H and X_L were performed for other dates and stations, respectively, and the results show that series X_H and X_L all well satisfy the Gaussian distribution. It is worth emphasizing that all theoretical analyses about RB temperature events in this paper are based on the premise that series X_H and X_L are subject to the Gaussian distribution.

3.3 Probability distribution for RB events

We still use the terminology of high temperatures, but the same formulism applies for low temperatures. The probability density function of series X_H subject to the Gaussian distribution is (Render and Petersen, 2006)

$$P(T) = \frac{1}{\sqrt{2\pi\sigma^2}} e^{-T^2/2\sigma^2}, \quad (10)$$

where T is the anomaly of daily maximum temperature, and σ is the standard deviation of series X_H .

Because series X_H are all anomaly values, $T_0 = 0$. Substituting Eq. (10) and $T_0 = 0$ into Eq. (2), and then integrating Eq. (2) by a substitution of dT with du and $u = T^2/2\sigma^2$ yields the expected value of the intensity of RB high temperature events:

$$\begin{aligned} T_1 &= \frac{\int_0^\infty \frac{\sigma}{\sqrt{2\pi}} e^{-u} du}{\frac{1}{2} \operatorname{erfc}(0)} = \sqrt{\frac{2}{\pi}} \sigma, \\ T_2 &= \frac{\int_{T_1}^\infty \frac{1}{\sqrt{2\pi\sigma^2}} T e^{-T^2/2\sigma^2} dT}{\int_{T_1}^\infty \frac{1}{\sqrt{2\pi\sigma^2}} e^{-T^2/2\sigma^2} dT} = \frac{T_1 e^{-T_1^2/2\sigma^2}}{\operatorname{erfc}(T_1/\sqrt{2\sigma^2})}, \\ &\dots, \\ T_k &= \frac{\int_{T_{k-1}}^\infty T \frac{1}{\sqrt{2\pi\sigma^2}} e^{-T^2/2\sigma^2} dT}{\int_{T_{k-1}}^\infty \frac{1}{\sqrt{2\pi\sigma^2}} e^{-T^2/2\sigma^2} dT} \\ &= \frac{\int_{T_{k-1}^2/2\sigma^2}^\infty \frac{\sigma}{\sqrt{2\pi}} e^{-u} du}{\frac{1}{2} \operatorname{erfc}(T_{k-1}/\sqrt{2\sigma^2})} \\ &= \frac{\sqrt{\frac{2}{\pi}} \sigma e^{-T_{k-1}^2/2\sigma^2}}{\operatorname{erfc}(T_{k-1}/\sqrt{2\sigma^2})}. \end{aligned} \quad (11)$$

Moreover, T_k can be briefly written by using

$$T_1 = \sqrt{\frac{2}{\pi}} \sigma \text{ as} \quad T_k = \frac{T_1 e^{-T_{k-1}^2/2\sigma^2}}{\operatorname{erfc}(T_{k-1}/\sqrt{2\sigma^2})}, \quad (12)$$

where $\operatorname{erfc}(z)$ is the supplementary error function, and its value depends only on z . If the standard deviation σ of the Gaussian distribution of series X_H is determined, then T_1 can be obtained from Eq. (11), and the theoretical value, i.e., T_2, T_3, \dots, T_k , of RB high temperature events can be determined by using recursive relation expressed by Eq. (12). Therefore, it is known from Eq. (12) that the theoretical value of T_k is only related to the standard deviation of Gaussian distribution. If the standard deviation of series X_H for a specified day is known, the theoretical value of T_k for that day can be computed.

If T_1 is known, i.e., computed from Eq. (11), then T_2, T_3, \dots, T_k can be obtained recursively by using Eq. (12):

$$\begin{aligned} T_2 &= \frac{\sqrt{\frac{2}{\pi}} \sigma e^{-(\sqrt{\frac{2}{\pi}} \sigma)^2/2\sigma^2}}{\operatorname{erfc}((\sqrt{\frac{2}{\pi}} \sigma)^2/2\sigma^2)} \\ &= \frac{e^{-1/\pi}}{\operatorname{erfc}(1/\pi)} T_1 \approx 1.712 T_1, \\ T_3 &= \frac{T_1 e^{-T_2^2/2\sigma^2}}{\operatorname{erfc}(T_2^2/2\sigma^2)} \approx 2.188 T_1, \\ T_4 &\approx 2.782 T_1, \dots \end{aligned} \quad (13)$$

In terms of $T_1 = \sqrt{\frac{2}{\pi}} \sigma$, the parameter of the denominator of Eq. (12) can be written as $T_k/\sqrt{2\sigma^2} = \frac{(T_k/T_1)}{\sqrt{\pi}}$. Generally, when $k \geq 3$, $\frac{(T_k/T_1)}{\sqrt{\pi}}$ will be greater than 1, so the supplementary error function may be written in an asymptotic form:

$$\operatorname{erfc}(z) \sim \frac{e^{-z^2}}{z\sqrt{\pi}} \left(1 - \frac{1}{2z^2} + \dots\right). \quad (14)$$

Substituting Eq. (14) into Eq. (12) yields

$$\begin{aligned} T_{k+1} &= \frac{T_1 e^{-T_k^2/2\sigma^2}}{\operatorname{erfc}(T_k/2\sigma^2)} \\ &\sim \frac{T_1 e^{-T_k^2/2\sigma^2}}{\sqrt{\frac{2\sigma^2}{\pi T_k^2}} e^{-T_k^2/2\sigma^2} \left(1 - \frac{1}{2(T_k/2\sigma^2)} + \dots\right)} \\ &\sim T_k \left(1 + \frac{\sigma^2}{T_k^2}\right), \end{aligned} \quad (15)$$

and its approximation form can be written as

$$T_{k+1} - T_k = \sigma^2/T_k. \quad (16)$$

It can be seen from Eq. (16) that with increasing k , the difference between two successive RB high temperature events will become smaller and smaller. After derivation, integration, and exhausting computations of difference approximation, the following simple form of the approximation of intensity of the k th RB high temperature event was obtained:

$$T_k \sim \sqrt{2k\sigma^2}. \quad (17)$$

Obviously, the conclusion of Eq. (17) is based on the assumption that the daily temperature distribution can be approximately described by the Gaussian distribution, and is a result in the statistical sense, i.e., an extreme value in the mean state, rather than the intensity of a specific RB event. It indicates that with the increase of k , the intensity of RB event is positively proportional to $\sqrt{2k\sigma^2}$.

Based on the series X_H at Nanjing station, Fig. 3 gives a comparison of actual RB high temperature events with their theoretical values obtained from Eq. (17). Figure 3 verified the reasonability of Eq. (17). Results from other stations are similar to Nanjing (figures omitted). According to Eq. (17), the k th record high temperature event intensity T_k is positively proportional to $\sqrt{2k\sigma^2}$. To obtain a physical quantity of statistical sense, values of T_k/σ for each day were computed at first, and then averaged. Figure 3 shows

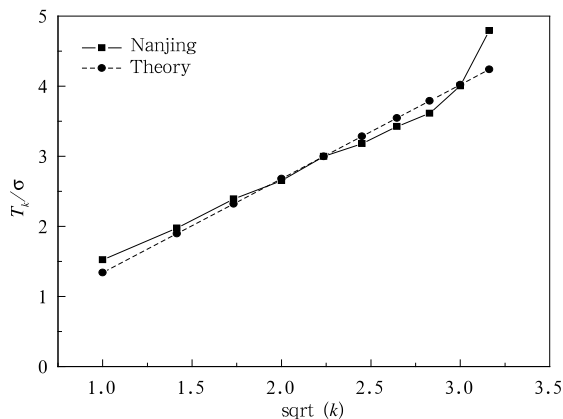


Fig. 3. Average k th record high temperature for each day (solid line), divided by the daily temperature dispersion, versus k (from the Nanjing temperature data). The theory curve is $T_k/\sigma \sim 1.34\sqrt{k}$ (dashed line).

that there is a linear statistical relation between T_k/σ and k . Although the actual value of T_k/σ fluctuates around the theory value, the deviations of the both are small, thus verifying the validity of the theoretic model of the RB extreme temperature events, meanwhile suggesting that meteorological variable extreme events still abide by certain evolutionary laws. Therefore, Eqs. (12) and (17) can be used to predict the intensity of future RB events.

4. Results

4.1 Standard deviations of series X_H / X_L

Because the theoretic values of T_k are only related to the standard deviations of series X_H and X_L , studies on the annual variation of T_k and the spatial distribution of the standard deviation of various stations over China are of application values. Standard deviation is a statistical parameter, which is used to assess the difference of a specified value in a group of values from the mean of the group, and to assess the change and fluctuation extents of the value. The larger the standard deviation of temperature series, the larger the fluctuations and waves of temperature. Figure 4 displays the annual variations of the standard deviations of series X_H and X_L of Nanjing. It can be seen from Fig. 4 that the standard deviations are larger in winter and smaller in summer for both series X_H and X_L , indicating that the amplitude of daily temperature change in winter is larger than that in summer.

Because extremely high/low temperature events always occur in summer/winter, the RB high/low temperature events in summer/winter are paid more attention to than that in other seasons. We computed the standard deviations of daily maximum temperature at 583 stations for each day in summer, which were then averaged over summer for each station, respectively, yielding the summer mean of the standard deviation of daily high temperature for each of the 583 stations. Likewise, the winter mean of the standard deviation of daily low temperature for each of 583 stations was also obtained. Figure 5 shows the pattern of the summer (winter) mean standard deviation of daily maximum (minimum) temperature. The summer mean standard deviation (Fig. 5a) exhibits a better organized zonal pattern gradually reducing from north to south, with the largest values in the

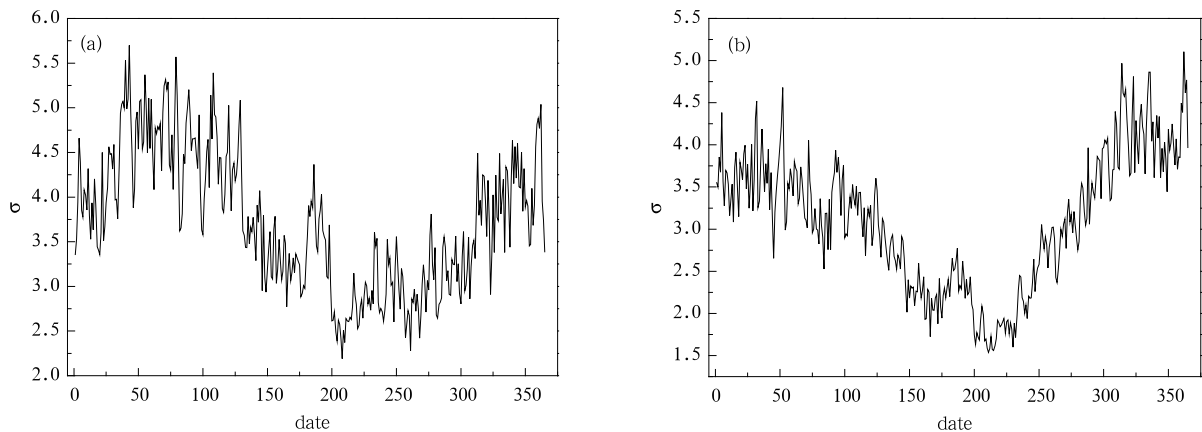


Fig. 4. Annual variations of the standard deviations of the daily extreme temperature series at Nanjing for (a) X_H and (b) X_L , averaged over the period of 1960–2005.

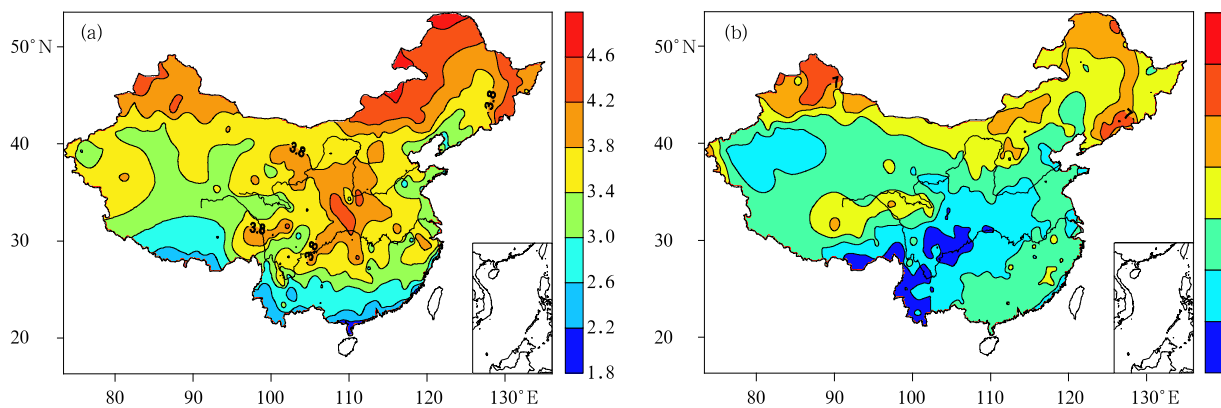


Fig. 5. Distributions of standard deviations of (a) summer mean daily maximum and (b) winter mean daily minimum temperatures over China for 1960–2005.

east of Inner Mongolia, the north of Heilongjiang, and the north of Xinjiang, and large values in the Chongqing-Shaanxi-Ningxia-Shanxi-Henan area; while most of southern China and the south of Xizang are minimum value areas. In contrast, the winter mean standard deviation (Fig. 5b) shows no zonal patterns, and Northeast China and the north of Northwest China are still larger value areas. However, in Southwest China and Central China, where the summer-mean standard deviation is larger (i.e., the fluctuation of daily maximum temperature in summer is larger), the fluctuation of daily minimum temperature in winter is smaller. Besides, it is also smaller in the southwest of Xinjiang, but larger in the southeast coastal regions such as Guangdong and Guangxi provinces.

4.2 Intensity and occurrence time of RB temperature events

Figure 6 shows distributions of historical maxi-

imum and minimum temperatures observed at 583 stations over China from 1960 to 2005. It is seen from Fig. 6a that the historical high temperature shows large regional differences, and there are three major high temperature belts in China. The first belt lies in most of Xinjiang and the west of Inner Mongolia, where the extremely high temperature of 47.7°C occurs. The second major high temperature belt with a historical record of greater than 40°C, occupies a large range, extending from Chongqing northwestwards to Northeast China, up to the west of Heilongjiang, covering Inner Mongolia, Beijing, Hebei, Shanxi, Shandong, Shaanxi, Hubei, Anhui, Chongqing, etc. The third high temperature belt with a historical extremely high temperature greater than 40°C is located in the south of Zhejiang, Fujian, Jiangxi, Hunan, and part of Guangxi. A small value area of historical extremely high temperature lies in the south of Qinghai and most of Xizang, with the smallest value of 19.3°C in Pali

of Xizang. The historical extremely low temperature (Fig. 6b) shows a distinctive zonal distribution in most of China except the Qinghai-Xizang Plateau. It generally reduces from north to south, with the highest value in South China and the lowest value in the north of Northeast China.

To predict the intensity of future RB high/low temperature on a specific day at a specific station, the actual number k of RB high/low temperature in 1960–2005 was first counted, future (after 2005) first time RB high/low temperature event should be the $(k+1)$ th event. A series of the theoretical expected values of RB high/low temperature were iteratively calculated using Eq. (12) and T_0 . Because it is in fact an anomaly, the intensity value of the $(k + 1)$ th event should be the anomaly plus the corresponding mean value at the station for that day. After the completion of the above computation for each day of 365 days at the station, we selected the largest/smallest one from the 365 computed future first RB high/low temperature events as the predicted value of this station.

Shown in Figs. 7a and 7b are the expected values of future first RB high and low temperatures predicted by using Eq. (12) and T_0 . It is seen that the predicted values overall accord with observed historical records (Fig. 6), but there are still some problems. For example, predicted values of future first RB high temperatures at some stations are smaller than corresponding historical observations, which is in no doubt unreasonable. Similar circumstances occurred for RB low temperatures. The reason for this might be that the computation of the theoretically predicted val-

ues did not take the real RB high/low temperatures into account. To be specific, in the above iterative computation of the theoretical expectation values of RB high/low temperatures T_1, \dots, T_{k+1} by using Eq. (12), theoretical values, $T_1 = \sqrt{\frac{2}{\pi}}\sigma, T_2, \dots, T_k$ instead of the real values $T_{1r}, T_{2r}, \dots, T_{kr}$, were used in the lower limit of the integral, respectively, and the deviation between the real and the theoretical values in the multiple iterations was not effectively corrected, which at last resulted in the occurrence of the unreasonable prediction. To solve this problem, the intensity value T_{kr} of the k th real (observed) RB event was used at each iteration to replace the theoretical value T_k as the initial condition. Equation (12) becomes Eq. (18):

$$T_{k+1} = \frac{\sqrt{2/\pi}\sigma e^{-T_{kr}^2/2\sigma^2}}{\operatorname{erfc}(T_{kr}/\sqrt{2\sigma^2})}. \quad (18)$$

The accuracy of Eqs. (18) and (12) was examined by the hindcast of historical maximum temperature at various stations. Figures 8a and 8b give distributions of historical high temperatures hindcasted by using Eqs. (18) and (12), respectively. It can be seen from comparing Fig. 8 with Fig. 6a that there are also three high temperature belts in Fig. 8a, which is consistent with Fig. 6a, but the second high temperature belt does not extend northeastwards up to Northeast China as in the observation (Fig. 6a), but up to the Beijing area. The other two high temperature belts in Fig. 8a accord well with those in Fig. 6a. Differences between Fig. 8b and Fig. 6a are relatively large. Therefore, the prediction of T_{k+1} obtained by using

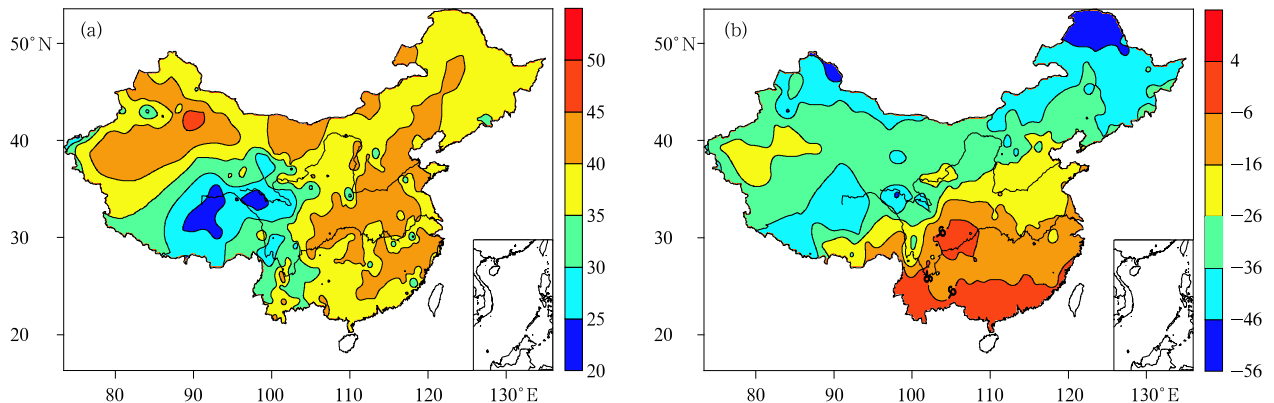


Fig. 6. Distributions of observed historical extremely (a) high and (b) low temperatures over China in 1960–2005.

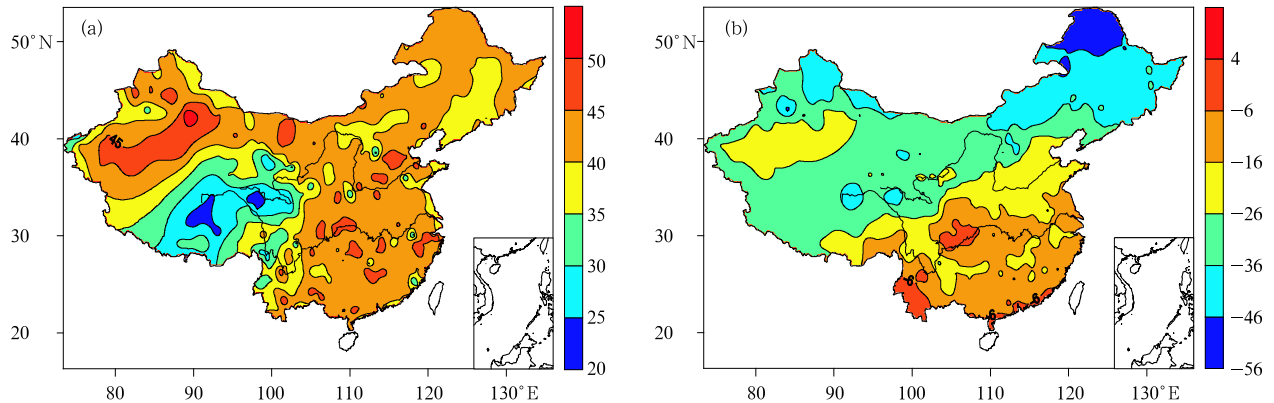


Fig. 7. Distributions of theoretically predicted values of future first RB (a) high and (b) low temperatures over China.

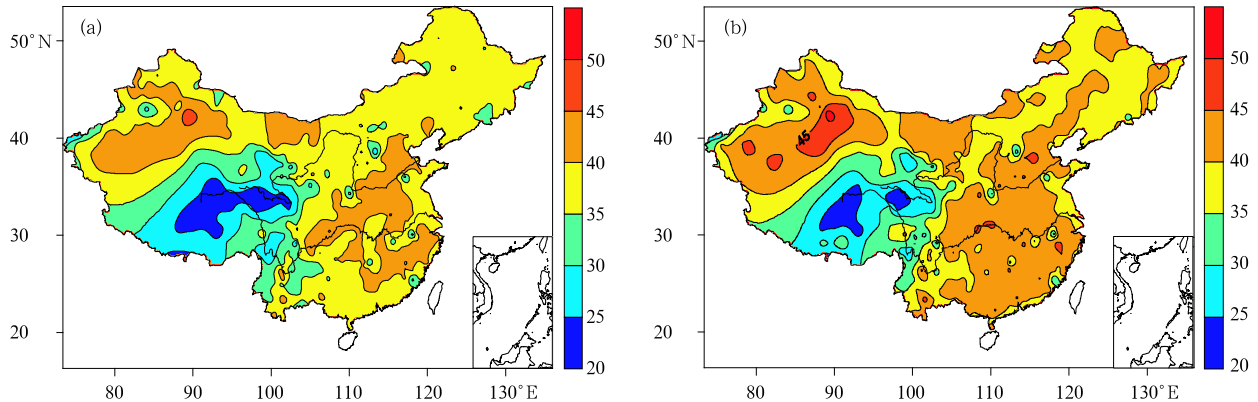


Fig. 8. Distributions of historical high temperatures hindcasted using (a) real value T_{kr} (Eq. (18)) and (b) theoretical value T_k (Eq. (12)) as the initial condition for the integral computation of T_{k+1} .

the real value T_{kr} as the initial condition for the iteration computation is closer to the real value than that obtained by using the theoretical value T_k . This also suggests from another angle that the prediction of extreme events is not easy.

Figure 9 shows predicted values of future first RB extreme temperatures by Eq. (18). The area of future extreme high temperature greater than 40°C expands, and the original two high temperature belts over eastern China merge into a large one, forming the most important warming area of China. The large value center of RB high temperatures $> 50^{\circ}\text{C}$ is still in Xinjiang, and the intensity value of future RB high temperature event in the Qinghai-Xizang Plateau as a cold source area is about 25°C , a very small value relative to other areas. The future RB low temperature there (Fig. 6b) is less than -55°C . The pattern of future RB low temperature (Fig. 9b) accords well

with the pattern of historical records (Fig. 6b), but with reduced values and with the lowest value center still in the north of Northeast China and around the Qinghai-Xizang Plateau.

Aimed at facilitating intuitive understanding of changes, Fig. 10 gives the positive/negative increments of future first RB high/low temperatures over the corresponding historical records. It can be seen from Fig. 10a that the increased amplitude of the high temperature is greater than 1°C in most of China, and there are three areas of larger values: the north of Yunnan to the south of Sichuan and part of Guizhou area with the largest value of about 2.5°C ; the Shaanxi-Henan-Shanxi area with the largest value of 2.0°C ; and the west of Inner Mongolia to the east of Heilongjiang and part of Jilin with the largest increased amplitude of 1.5°C . The area of the smallest value lies in the southeast coastal region, and the increased amplitude

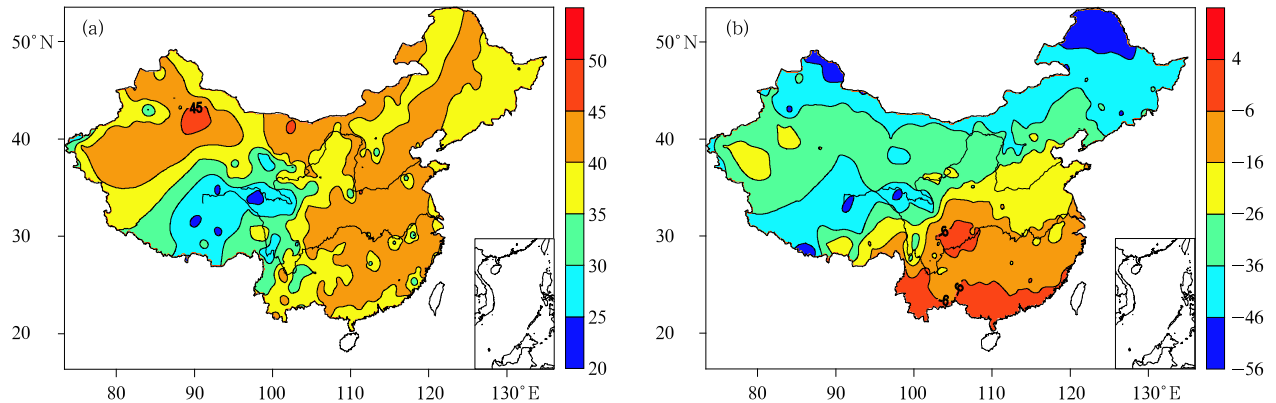


Fig. 9. Distributions of future first RB (a) high and (b) low temperatures predicted by Eq. (18).

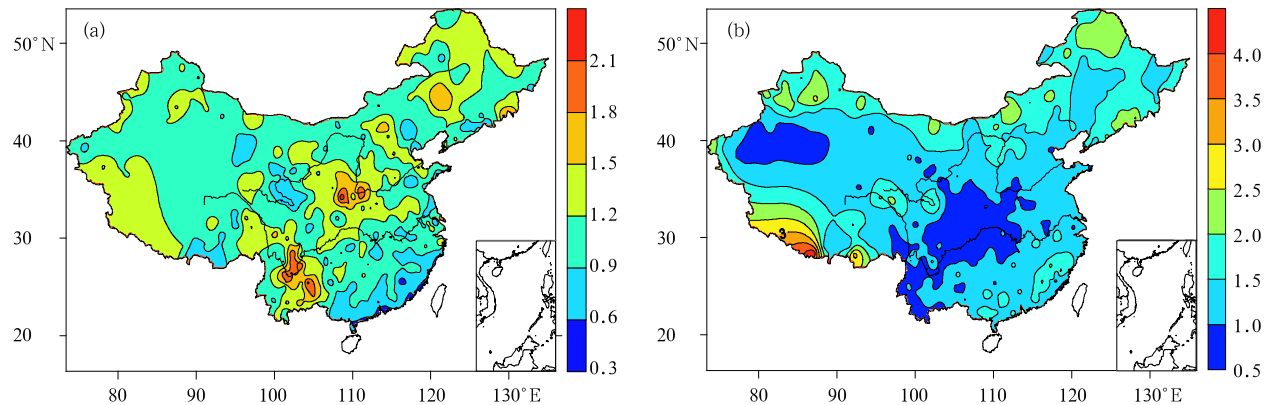


Fig. 10. Increments of future first RB high (a) and low (b) temperatures relative to the historical extreme high and low temperatures.

is only about 0.5°C . As for future first RB low temperature (Fig. 10b), the area with the largest decrease lies in the south of Xizang, with the largest decline of 4°C ; the medium decrease is seen sporadically in the southeast coastal region and higher latitude regions north of 40°N , with a decreased amplitude of about 2.5°C ; two small value areas lie in Chongqing, most of Sichuan, and the west of Yunnan-Hunan-Hubei-Shaanxi and part of Gansu area, and the southwest of Xinjiang, respectively, where the maximum decreased amplitude is mostly about 0.5°C ; and the decreased amplitudes in the rest areas are more uniformly between 1 and 2°C . Distributions of the predicted values of increments given in Fig. 10 reflect spatial changes of the intensity of future first RB high/low temperature events. On the other hand, their occurrence time is also concerned. Figure 11 displays frequencies of historical RB high/low temperature events for different days (1, 2, ..., 365) in 1960–2005 at Nanjing station.

The results at other stations are similar (figures omitted). During the 46 yr, on some days, eight high or seven low temperature RB events occurred, while on other days only one high or low temperature RB event occurred; the difference in the event frequency is large.

Equation (9) gives the time interval between two successive RB temperature events. To predict the occurrence time of future first RB high (low) temperature event at a station on a specific day, Eq. (9) is first used to calculate the time interval between the last occurred (k th) RB high (low) temperature event and future first (k th) RB high (low) temperature event, and then the actual occurrence time of the k th high (low) temperature event is added to the time interval derived. According to Eq. (9), the theoretical occurrence time of future first RB event is

$$t_{k+1} = \frac{2}{\text{erfc}(T_{kr}/\sqrt{2}\sigma^2)} + t_{kr}, \quad (19)$$

where T_{kr} and t_{kr} denote the intensity of the last (k th) RB event and its actual occurrence time, respectively.

Equation (19) was used to calculate the occurrence time of future (after 2005) first RB high/low temperature events for each of the 583 stations and each day of the year. Their average predicted time (year) is plotted in Figs. 12a, b. The earliest occurrence time for the high temperature event (Fig. 12a) lies in southern China, especially in the east of Yunnan, Guangdong, and part of Guangxi, and the average occurrence time in Hubei, Shaanxi, and part of Xinjiang is also earlier, indicating that those are areas where future RB high temperature events will be frequent. The average occurrence time for the high temperature events in the Jiangsu-Zhejiang area, Inner Mongolia, Heilongjiang, and most of the Qinghai-Xizang Plateau will be about 2100, suggesting that under the condition of regional climate change, the current extremely high temperature events in those

areas have reached a higher level, and thus it is relatively difficult to break the current record. The occurrence time in most of the rest areas will be about 50–75 yr later. The spatial distribution of the average occurrence time of future (after 2005) first RB low temperature events (Fig. 12b) is just opposite to that of the high temperature events. The average occurrence time is later in areas of Southwest China and Guangdong where future RB high temperature events are frequent; while it is earlier in Northeast China where the average occurrence time for high temperature events is later. Overall, the average occurrence time of future first RB low temperature events is later than that of the high temperature events; it is about 100 yr later, and at least 50 yr later in most areas of China. Therefore, it can be seen from the above analysis that the extremely high temperature events will dominate the extreme events in the future 100 years. This conclusion is also in accordance with the current

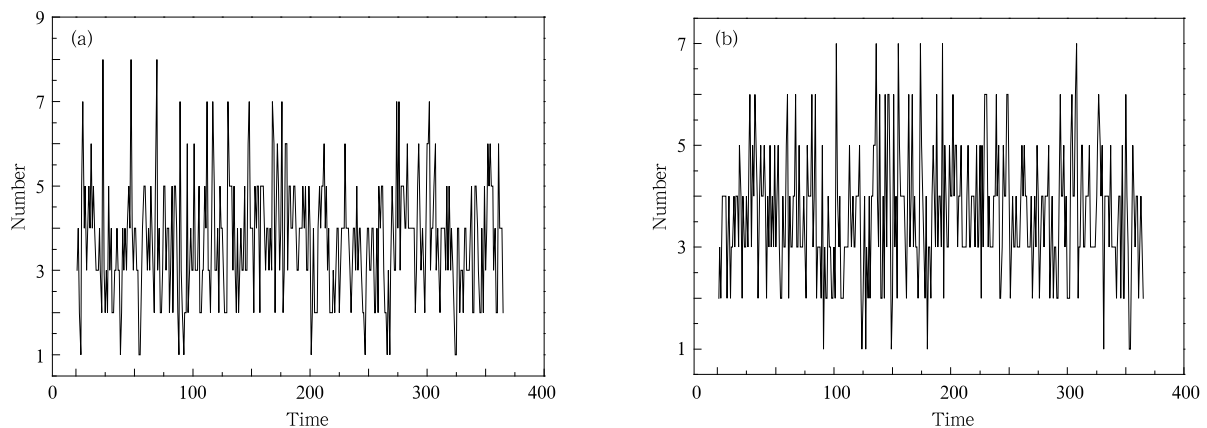


Fig. 11. Numbers of the RB events for daily (a) high and (b) low temperatures at Nanjing station in 1960–2005.

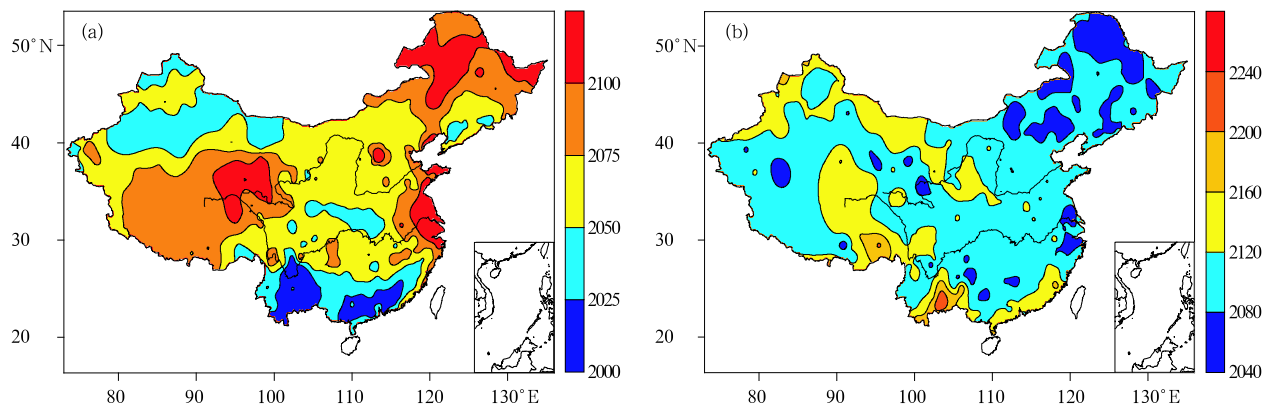


Fig. 12. Distributions of the average predicted occurrence time (year) of the future first RB (a) high and (b) low temperature events.

fact of the globally rising average temperature (Wang et al., 1998; Gong et al., 2006b).

4.3 Saturation values of RB temperature

In Subsection 4.2, we have given the predicted values of future first RB high/low temperature, which show the intensity augment and area expansion of future extreme temperatures. However, in reality, the high/low temperature records could not be broken successively, i.e., temperature has its upper and lower limits. In Subsection 3.3, we have discussed that with increasing k , the increased amplitude of the intensity of extreme events will gradually become small, and be saturated at last. To take this point into account, we consider that when the difference between T_{k+1} and T_k is very small, i.e.,

$$\left| \frac{(T_{k+1} - T_k)}{T_k} \right| \leq 0.01. \quad (20)$$

The increments of T_{k+1} relative to T_k can be neglected, and the intensity of RB events has reached its limit (the saturation value equals T_{k+1} plus the corresponding mean).

The saturation values of RB high/low temperature were calculated based on Eq. (20) for each of 583 stations, and the results were plotted in Figs. 13a, b. It can be observed from Fig. 13a that the saturation value is greater than 50°C in most of China except the Qinghai-Xizang Plateau, with two large value centers of above 60°C in the Turfan Basin and the border of Yunnan, Guizhou, and Guangxi, respectively; while the theoretical saturation value of high temperature in

the plateau area, where temperature is lower over the whole year, is only about 30°C . As for the saturation value of RB low temperature (Fig. 13b), two lowest value centers with a value of -75°C lie in the plateau and the north of Northeast China; and except a higher value region in Chongqing and the east of Sichuan, the saturation value overallly shows a zonal distribution, with its value gradually reducing from south to north.

Figure 14 displays the maximum increase/decrease (the theoretical saturation value minus the corresponding observed record) of the future RB high/low temperature events. The maximum increases (Fig. 14a) are concentrated in two areas: one is Northwest China and most of the Qinghai-Xizang Plateau, where the spacial coverage of the increase of high temperature is small; and the other is Central China, East China, Northeast China, North China, and the Yunnan-Guizhou Plateau, where the spatial coverage of the increase of high temperature is large. The extremely high temperature at present is far from saturation, especially in the border between Yunnan and Guizhou and part of Guangxi, where the spatial coverage of the increase is the largest and the theoretical increase may reach above 20°C . The distribution of the maximum decrease of the RB low temperature events (Fig. 14b) is relatively complicated. There are two remarkably cooling areas: one is most of northern China, especially the east of Liaoning, Heilongjiang, the north of Inner Mongolia, and the north of Xinjiang, where the spatial coverage of the decrease of extremely low temperature is large; and the other is the southeast coastal region, where the spatial coverage of the

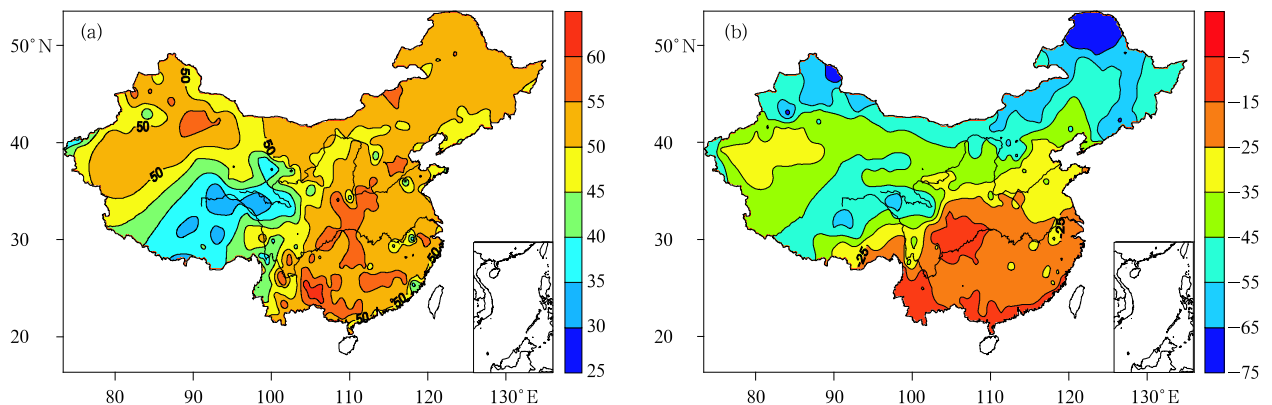


Fig. 13. Distributions of the saturation values ($^\circ\text{C}$) of the RB (a) high and (b) low temperature events over China.

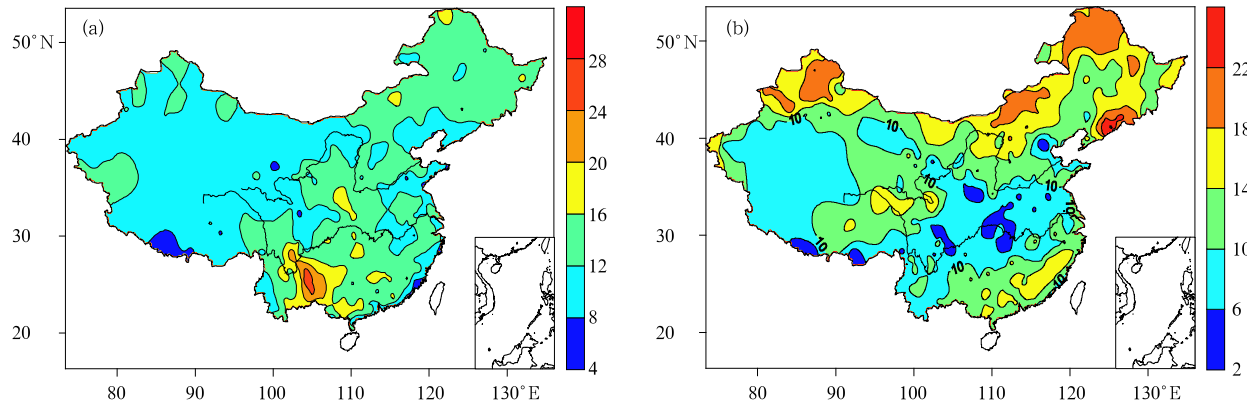


Fig. 14. Distributions of the maximum theoretical increase and decrease ($^{\circ}\text{C}$) of the future RB (a) high and (b) low temperature events over China.

decrease of extremely low temperature is also large. The smaller decrease area lies in Southwest China and Central China, especially in Hubei, Chongqing, and part of Shaanxi, where the maximum decrease is only about 5°C . Therefore, the decrease of the future extreme low temperature events exhibits a sandwich pattern in space.

The areas with larger spatial coverages of increase/decrease of the RB high/low temperature cover almost all major economic zones, natural and ecological reserves of China, among which Northeast China and South China are major grain production bases, and the southeast coastal region is currently the most important industry base. The exacerbation of extreme high/low temperature events will no doubt affect greatly the industrial and agricultural production in those areas (Chen et al., 2003; Gong et al. 2006b). North China is one of the ecologically most vulnerable areas in China, and also the place of China's capital. The Yunnan-Guizhou Plateau is a region where tropical rainforests and ecological species are best reserved in China or even in the world. With the development of national economy and urbanization and the growth of population in cities, the increased exacerbation of extremely high/low temperature events will greatly influence the environment, people's life, and the social stability. All these are strategic problems that need to be urgently studied and solved (Gong and Han, 2004; IPCC, 2007).

5. Conclusions

The 1960–2005 daily maximum/minimum tem-

perature data at 583 stations, where the temperature record is complete, have been used in this study to explore the occurrence regularity of RB temperature events in China in the past 46 years. The probability density functions of series X_H and X_L have been verified to be approximate of Gaussian normal distributions. Based on the above premise, predicted values of RB extreme temperature events were calculated. The results show that predicted values by the Gaussian model based on the initial condition of observed RB high/low temperature events are more reasonable and closer to the corresponding observations than those based on the initial condition of expected values of RB high/low temperatures. The spatial pattern of future RB high temperature events will change to some extent in comparison with the current observed pattern. The most remarkable change is a further expansion of the area of RB high temperatures above 40°C , especially in central Northeast China and Southwest China (e.g., Guangxi). This accords with the distribution of the future increase of the RB high temperature events, i.e., the expanded areas just match the areas where the future increases are larger. In contrast to high temperature, the spatial distribution of the RB low temperature events is stable relative to the historical low temperature pattern, but the intensity of the future low temperature events will augment, with the largest decrease in the south of Xizang and smaller decreases in most of the rest areas.

The earliest average occurrence time for the future RB high temperature events lies in Southwest China and part of Guangdong, where the future

RB high temperature events are frequent. While the latest average occurrence time will be located in the Jiangsu-Zhejiang area, most of Northeast China, and part of the Qinghai-Xizang Plateau. On the contrary, the average occurrence time of the future RB low temperature events will be generally later than that of the high temperature events. The extremely high temperature event will dominate the extreme events in the future 100 years, which is in accordance with the current fact of global warming.

The distributions of maximum theoretical increase/decrease of the RB high/low temperature for the 583 stations show that except Northeast China where the spatial coverage of the increase of the high temperature events will be smaller, there will be a larger expansion in most of the rest areas in China, especially in Southwest China. As for the low temperature events, there will be a larger decreasing area in Northeast China and most of the southeast coastal region, while in Southwest China and Central China, the decreasing range will be smaller; thus overall displaying a sandwich pattern.

REFERENCES

- Beniston, M., D. B. Stephenson, O. B. Christen, et al., 2007: Future extreme events in European climate: An exploration of regional climate model projections. *Climate Change*, **81**(Suppl. 1), 71–95.
- Chen Bingyan, Ding Yuguo, and He Juanxiong, 2003: The influence of global warming on probability of regional extreme temperatures. *J. Trop. Meteor.*, **19**(4), 429–435. (in Chinese)
- Deng Ziwang, Ding Yuguo, and Chen Yeguo, 2000: Effects of global warming on the probability of extreme high temperature events in the Yangtze Delta. *J. Nanjing Inst. Meteor.*, **23**(1), 42–47. (in Chinese)
- Ding Yihui, Ren Guoyu, Zhao Zongci, et al., 2007: Detection, attribution and projection of climate change over China. *Desert Oasis Meteor.*, **1**(1), 1–10. (in Chinese)
- Ding Yuguo, Liu Jifeng, and Zhang Yaocun, 2004: Simulation tests of temporal-spatial distributions of extreme temperatures over China based on probability weighted moment estimation. *Chinese. J. Atmos. Sci.*, **28**(5), 771–782. (in Chinese)
- Feng Guolin, Dong Wenjie, Gong Zhiqiang, et al., 2006: *Nonlinear Theories and Methods on Spatial-Temporal Distribution of the Observational Data*. China Meteorological Press, Beijing, 1–227. (in Chinese)
- Fu Congbin and Ye Duzheng, 1995: Global change and the future trend of ecological environment evolution in China. *Chinese J. Atmos. Sci.*, **19**(1), 116–126. (in Chinese)
- Gong Daoyi and Han Hui, 2004: Extreme climate events in northern China over the last 50 years. *Acta Geographica Sinica*, **59**(2), 230–238. (in Chinese)
- Gong Zhiqiang, Feng Guolin, Wan Shiquan, et al., 2006a: Analysis of features of climate change of Huabei area and the global climate change based on heuristic segmentation algorithm. *Acta Phys. Sinica*, **55**(1), 477–484. (in Chinese)
- , —, Dong Wenjie, et al., 2006b: The research of dynamic structure abrupt change of nonlinear time series. *Acta Phys. Sinica*, **55**(6), 3180–3187. (in Chinese)
- Hou Wei, Feng Guolin, Dong Wenjie, et al., 2006: A technique for distinguishing dynamical species in the temperature time series of North China. *Acta Phys. Sinica*, **55**(5), 2663–2668. (in Chinese)
- IPCC, 2007: *Climate Change 2007: The Physical Science Basis*. Contribution of Working Group I to the Fourth Assessment Report of the Intergovernmental Panel on Climate Change. Cambridge University Press, Cambridge United Kingdom, and New York, USA.
- Kiktev, D., D. M. H. Sexton, L. Alexander, et al., 2003: Comparison of modeled and observed trends in indices of daily climate extremes. *J. Clim.*, **16**(22), 3560–3570.
- Liu Jifeng, Li Shijie, Ding Yuguo, et al., 2006: The discussion of the characteristic zoning method of extreme temperature in China in recent decades. *J. Mountain Sci.*, **24**(3), 201–297. (in Chinese)
- Liu Shida, Rong Pingping, and Chen Jiong, 2000: The hierarchical structure of climate series. *Acta Meteor. Sinica*, **58**(1), 111–114. (in Chinese)
- Qin Dahe, Chen Zhenlin, Luo Yong, et al., 2007: Updated understanding of climate changes. *Adv. Climate Change Res.*, **1**(1), 1–10. (in Chinese)
- Render, S., and M. R. Petersen, 2006: Role of global warming on the statistics of record breaking temperatures. *Phys. Rev. E.*, **74**, 061114.

- Sugihara, G., and R. M. May, 1990: Nonlinear forecasting as a way of distinguishing chaos from measurements error in time series. *Nature*, **344**, 734–741.
- Wan Shiquan, Feng Guolin, Zhou Guohua, et al., 2005: Extracting useful information from the observations for prediction based on EMD method. *Acta Meteor. Sinica*, **63**(4), 516–525. (in Chinese)
- Wang Shaowu, Ye Jinlin, Gong Daoyi, et al., 1998: Construction of mean annual temperature series for the last one hundred years in China. *Quart. Appl. Meteor. Sci.*, **9**(4), 392–401. (in Chinese)
- Yang Peicai and Zhou Xiuji, 2005: On nonstationary behaviors and prediction theory of climate systems. *Acta Meteor. Sinica*, **63**(5), 556–570. (in Chinese)
- Ye Duzheng, Yan Zhongwei, Dai Xinggang, et al., 2006: A discussion of future system of weather and climate prediction. *Meteor. Mon.*, **32**(4), 3–8. (in Chinese)